




# Metabolic Synergy between Human Symbionts *Bacteroides* and *Methanobrevibacter*

Jennie L. Catlett,<sup>a</sup> Sean Carr,<sup>a</sup> Mikaela Cashman,<sup>b</sup> Megan D. Smith,<sup>a</sup> Mary Walter,<sup>a</sup> Zahmeeth Sakkaff,<sup>c</sup> Christine Kelley,<sup>d</sup> Massimiliano Pierobon,<sup>c</sup> Myra B. Cohen,<sup>c,e</sup>  Nicole R. Buan<sup>a</sup>

<sup>a</sup>Department of Biochemistry, University of Nebraska-Lincoln, Lincoln, Nebraska, USA

<sup>b</sup>Biosciences Division, Oak Ridge National Laboratory, Oak Ridge, Tennessee, USA

<sup>c</sup>Department of Computer Science & Engineering, University of Nebraska-Lincoln, Lincoln, Nebraska, USA

<sup>d</sup>Department of Mathematics, University of Nebraska-Lincoln, Lincoln, Nebraska, USA

<sup>e</sup>Department of Computer Science, Iowa State University, Ames, Iowa, USA

**ABSTRACT** Trophic interactions between microbes are postulated to determine whether a host microbiome is healthy or causes predisposition to disease. Two abundant taxa, the Gram-negative heterotrophic bacterium *Bacteroides thetaiotaomicron* and the methanogenic archaeon *Methanobrevibacter smithii*, are proposed to have a synergistic metabolic relationship. Both organisms play vital roles in human gut health; *B. thetaiotaomicron* assists the host by fermenting dietary polysaccharides, whereas *M. smithii* consumes end-stage fermentation products and is hypothesized to relieve feedback inhibition of upstream microbes such as *B. thetaiotaomicron*. To study their metabolic interactions, we defined and optimized a coculture system and used software testing techniques to analyze growth under a range of conditions representing the nutrient environment of the host. We verify that *B. thetaiotaomicron* fermentation products are sufficient for *M. smithii* growth and that accumulation of fermentation products alters secretion of metabolites by *B. thetaiotaomicron* to benefit *M. smithii*. Studies suggest that *B. thetaiotaomicron* metabolic efficiency is greater in the absence of fermentation products or in the presence of *M. smithii*. Under certain conditions, *B. thetaiotaomicron* and *M. smithii* form interspecies granules consistent with behavior observed for syntrophic partnerships between microbes in soil or sediment enrichments and anaerobic digesters. Furthermore, when vitamin B<sub>12</sub>, hematin, and hydrogen gas are abundant, coculture growth is greater than the sum of growth observed for monocultures, suggesting that both organisms benefit from a synergistic mutual metabolic relationship.

**IMPORTANCE** The human gut functions through a complex system of interactions between the host human tissue and the microbes which inhabit it. These diverse interactions are difficult to model or examine under controlled laboratory conditions. We studied the interactions between two dominant human gut microbes, *B. thetaiotaomicron* and *M. smithii*, using a seven-component culturing approach that allows the systematic examination of the metabolic complexity of this binary microbial system. By combining high-throughput methods with machine learning techniques, we were able to investigate the interactions between two dominant genera of the gut microbiome in a wide variety of environmental conditions. Our approach can be broadly applied to studying microbial interactions and may be extended to evaluate and curate computational metabolic models. The software tools developed for this study are available as user-friendly tutorials in the Department of Energy KBase.

**KEYWORDS** microbiome, *Bacteroides*, *Methanobrevibacter*, cross-feeding, synergy, metabolism, syntrophy

**Editor** Jan Claesen, Lerner Research Institute

This is a work of the U.S. Government and is not subject to copyright protection in the United States. Foreign copyrights may apply.

Address correspondence to Nicole R. Buan, nbuan@unl.edu.

The authors declare no conflict of interest.

**Received** 25 March 2022

**Accepted** 11 April 2022

**Published** 10 May 2022

From birth, the human microbiome plays an important role in maintaining human health (1–4). Newborns are colonized in their first days of life (5–7), and the microbiome grows and develops with the child into adulthood (5, 8). Depending on the age, geographic location, diet, and health of its host, 10 to 100 trillion microbial cells reside in the intestines alone (1, 9). These organisms are part of a dynamic, closely interconnected ecosystem made up of bacteria, archaea, and eukarya (7, 8, 10). Interactions between host-associated microbes affect many aspects of human health. A well-balanced, healthy microbiota offers protection against infection (11, 12), metabolizes nutritional compounds (13), provides essential vitamins and nutrients, adds 15 to 30% of human caloric intake (14, 15), manages weight gain (16), and influences the human immune system and its development (17–19). However, an unbalanced microbiome is linked to obesity, infections, asthma, allergies, Crohn's disease, irritable bowel disease, neurodegenerative disease, and cancer (1–4, 12, 17, 19–34).

It has been proposed that mutualistic relationships within the gut microbiome maintain a balance that is necessary for a healthy host digestive system (8, 29, 35). The dynamic interactions between microbes in a multispecies gut community are difficult to study both in the laboratory and using computational modeling and analysis due to the sheer complexity of the system. This complexity is due to many factors, including the combinatorial genetic space, sampling heterogeneity, unknown environmental conditions (e.g., local microvariation in temperature and pH and nutrient availability), and unknown relationships between interacting genetic and environmental variables that make it difficult to confidently ascribe major (or minor) organism functions in a mixed microbiome community. Fortunately, cutting-edge software system research approaches, such as statistical sampling and decision trees, can be used to develop tools for management and analysis of complex microbial systems (36). To benchmark new computational tools, we constrain the gut microbiome system to studying the relationship between two key human gut inhabitants: the fermenter *Bacteroides thetaiotaomicron* and the methanogenic archaeon *Methanobrevibacter smithii*.

*B. thetaiotaomicron* (*B. theta*) is one of the most prominent fermenters in the human gut, making up between 5 and 50% of the overall gut community (15). *B. theta* is a generalist fermenter: it consumes dietary plant polysaccharides such as starch as well as mucosal glycans such as heparin and produces fermentation products such as hydrogen, carbon dioxide, formate, acetate, and succinate (15). It plays a crucial digestive role by partially breaking down polysaccharides human cells are unable to degrade and produces short-chain fatty acids for human and microbial consumption (acetate, succinate, propionate, lactate). In the process, it protects intestines against infection by activating host immune defenses, through direct interactions, and by competition with other bacteria (12, 37).

*M. smithii* is the dominant methanogen in the human gut and makes up between 1% and 10% of the human gut community (38, 39). It colonizes the human gut in infancy, remains present in the majority of the population through adulthood (6, 38), and has been detected in up to 95.7% of individuals (39–42). Imbalance in *M. smithii* gut communities has been associated with obesity and malnutrition-related digestive diseases (2, 30, 41, 43). *M. smithii* is a hydrogenotrophic methanogen and can conserve energy through methanogenesis using carbon dioxide and hydrogen gas or formate as substrates (39, 44, 45). *M. smithii* has an incomplete reductive tricarboxylic acid (TCA) cycle and must assimilate acetate as a carbon substrate. It is hypothesized that growth of *M. smithii* in the gut could benefit *B. theta* and other fermenters by metabolizing fermentation products that would inhibit further fermentation by feedback inhibition as they accumulate. Moreover, the removal of hydrogen could allow *B. theta* to increase metabolic efficiency and contribute to effective metabolism of dietary substrates, since high hydrogen partial pressure inhibits bacterial NADH dehydrogenases, reducing the yield of ATP and causing fermentation overall to become endergonic (unfavorable) (35, 46). The proposed nature of the complementary metabolism between *B. theta* and *M. smithii* suggests a mutualistic relationship in which *M. smithii*

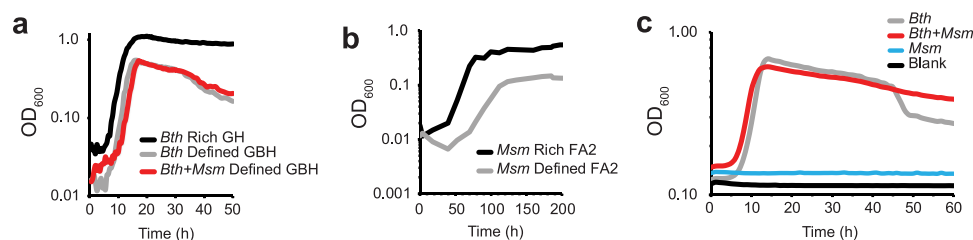


**FIG 1** Growth phenotypes on rich and defined culture media. (a) Growth of *B. theta* monocultures in anaerobic culture tubes in rich (black) or defined medium (gray) compared to *B. theta* plus *M. smithii* cocultures (red) grown on defined medium on 0.5% glucose ( $n = 5$ ). (b) Growth of *M. smithii* monocultures in anaerobic culture tubes in rich (black) or defined medium (gray) supplemented with 10 mM acetate and 10 mM formate under an atmosphere of 80%  $H_2$  ( $n = 5$ ). (c) Growth of *B. theta* (gray), *M. smithii* (blue), and *B. theta* plus *M. smithii* cocultures (red) on defined medium with 0.5% glucose as sole carbon and energy source in 96-well plates ( $n = 8$ ). Error bars have been omitted for clarity.  $OD_{600}$ , optical density at 600 nm. G, 0.5% glucose; B, vitamin  $B_{12}$  (cyanocobalamin); H, hematin; F, 10 mM formate; A, 10 mM acetate; 2, 80%  $H_2$  atmosphere.

relies on the metabolic products of *B. theta* fermentation to survive, while *B. theta* relies on *M. smithii* to remove products that would inhibit fermentation, which would be an example of metabolic syntrophy (46).

Syntrophy is a form of mutualism in which two organisms form a tightly coupled, mutually beneficial metabolic relationship (46–49). Syntrophic relationships allow bacteria to overcome energy barriers and to break down substrates more efficiently (35, 47, 49, 50). Methanogens have often been observed in syntrophic relationships with soil bacteria, removing hydrogen gas and other fermentation inhibitors to benefit the bacteria (46, 49, 51). *B. theta* and *M. smithii* have been previously proposed to form a syntrophic relationship based on genomic evidence (45). Gnotobiotic mouse studies suggest that the presence of *M. smithii* assists *B. theta* in the breakdown of polysaccharides and increases host digestive efficiency (35), and our previous study showed that feedback of *B. theta* is inhibited by acetate and formate (52), suggesting that a partner organism that consumes these metabolic by-products, such as *M. smithii*, may benefit *B. theta*. However, the relationship between *B. theta* and *M. smithii* is not fully characterized. One of the greatest obstacles is the difficulty in systematically identifying what conditions could lead to a synergistic metabolic relationship, such as syntrophy, that benefits both organisms.

To examine the metabolic relationship between *B. theta* and *M. smithii*, we established laboratory conditions in which both monocultures and cocultures of *B. theta* and *M. smithii* can be studied and characterized. We leverage an approach to test complex software, partitioning the input space and systematically manipulating program inputs and inferring interactions and relationships between the inputs. In the system we studied here, we observed organism and coculture growth behaviors as outputs dependent on culture nutrient inputs. We then devised an assay to compare monocultures and cocultures in 128 different nutrient conditions and evaluated growth using decision trees from machine learning to identify neutral, favorable, and unfavorable conditions for *M. smithii* and *B. theta* growing in coculture.

## RESULTS

### *B. theta* and *M. smithii* grow independently in both rich and defined media when supplemented with appropriate carbon sources.

Before we could examine the interactions between *B. theta* and *M. smithii*, we needed to understand how they grow separately in monocultures. The rich medium is based on a standard tryptone yeast extract recipe with high nutrient availability. In sealed anaerobic culture tubes supplemented with 0.05% glucose (Fig. 1a), *B. theta* doubled every 1.48 h (Table 1). Supplemented with 10 mM acetate and 10 mM formate under an atmosphere of 80%  $H_2$ , *M. smithii* grew at a much lower rate (Fig. 1b), with a doubling time of 8.8 h (Table 1). The difference in growth rates means that if two cultures are started at the

**TABLE 1** Culture doubling times (hours)<sup>a</sup>

Treatment	<i>B. theta</i> 0.05% glucose			<i>M. smithii</i> 10 mM acetate + 10 mM formate			Coculture 0.05% glucose			
	Maximum OD	Doubling time (SD)	<i>P</i> vs rich	Maximum OD	Doubling time (SD)	<i>P</i> vs rich	Maximum OD	Doubling time (SD)	<i>P</i> vs <i>B. theta</i>	<i>P</i> vs <i>M. smithii</i>
Anaerobic culture tube rich <sup>†</sup>	1.11 ± 0.013	1.48 ± 0.140	1	0.55 ± 0.051	8.84 ± 0.332	1	0.54 ± 0.020	1.46 ± 0.137	0.890	0.000
Anaerobic culture tube defined <sup>†</sup>	0.55 ± 0.017	1.40 ± 0.092	0.699	0.15 ± 0.007	15.46 ± 1.803	0.000	0.52 ± 0.016	1.44 ± 0.05	0.872	0.000
96-well plates rich <sup>†</sup>	0.64 ± 0.033	1.62 ± 0.097	1	0.17 ± 0.024	7.93 ± 0.825	1	0.745 ± 0.016	2.02 ± 0.073	0.001	0.000
96-well plates defined <sup>‡</sup>	0.69 ± 0.015	2.04 ± 0.100	0.000	0.14 ± 0.007	318 ± 23.13	0.000	0.61 ± 0.018	2.18 ± 0.067	0.030	0.000

<sup>a</sup>Data were collected from *n* = 5 (<sup>†</sup>) or *n* = 8 (<sup>‡</sup>) biological replicates. Significance *P* values were determined by unpaired Student's *t* test.

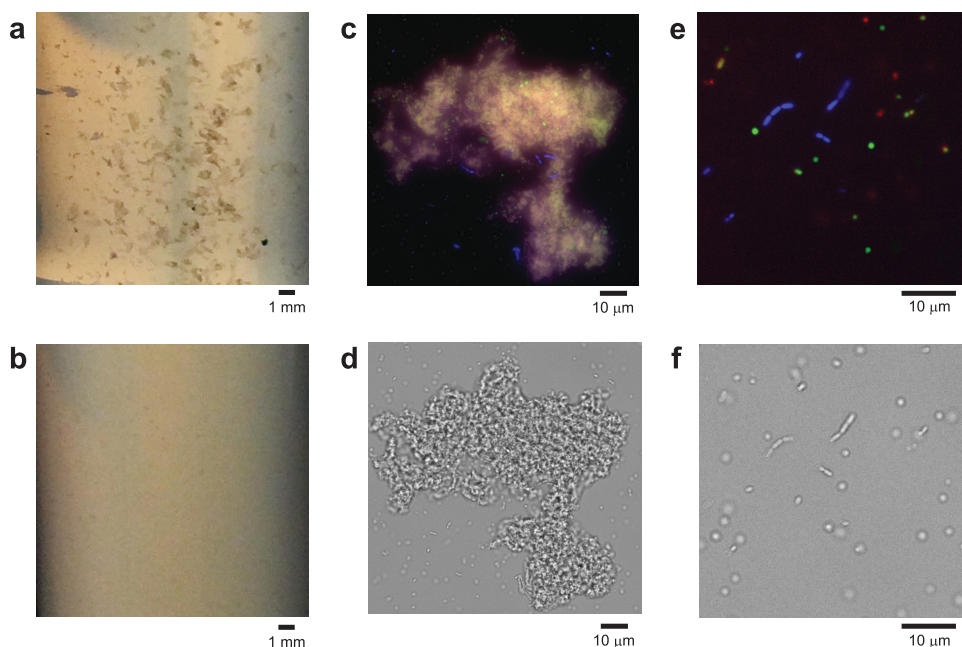


**FIG 2** Microscopy of *B.theta* and *M. smithii* in cocultures grown in rich medium for 8 days. (a) Coculture of *B.theta* and *M. smithii* grown on rich medium for 1 week showing visible aggregates. (b) Monoculture of *B.theta* grown on rich medium for 1 week. (c) Live/dead staining of a coculture aggregate appears to show that aggregates are comprised of live *B.theta* and *M. smithii* cells as well as what appears to be extracellular matrix and/or lysed cell debris. In live/dead micrographs, intact *B.theta* cells are green, intact *M. smithii* cells are blue, and dead cells are stained red. Yellow color results from colocalization of red and green channels. Methanogens autofluorescence due to oxidized coenzyme F<sub>420</sub> and appear blue when viewed under a DAPI LED light filter. (d) Transmission micrographs of panel c. (e) Live/dead staining of planktonic cells in coculture showing live *B.theta* (green), live *M. smithii* (blue), and dead cells (red). (f) Transmission micrograph of panel d. Black bars indicate scale.

same time, *B. theta* has already reached the stationary stage of growth when *M. smithii* is entering early log growth (Fig. 1a and b). In defined medium, the difference between *B. theta* and *M. smithii* monoculture growth is more pronounced. *B. theta* doubled every 1.4 h, while *M. smithii* doubled every 15.4 h (Fig. 1a and b, Table 1).

**The presence of *B. theta* is sufficient for *M. smithii* growth in cocultures.** In defined medium, optical density of cocultures was very similar to that of *B. theta* monocultures (Table 1) except culture density did not decrease after 50 h during stationary phase. A decrease in culture optical density may indicate a number of causes; among these are cell lysis or a change in cell shape or volume. The observation that cocultures did not show this decrease in optical density suggested that *M. smithii* protects *B. theta* from lysis, that it prevents a change in cell shape or volume, or that the optical density reflected growth of *M. smithii* even though *M. smithii* monocultures do not grow in medium lacking H<sub>2</sub> and CO<sub>2</sub> or formate and acetate (Fig. 1c). When cocultures were grown in rich medium in anaerobic culture tubes supplemented with 0.05% glucose, we observed aggregation of cells after 1 week of incubation (Fig. 2a). We did not observe aggregation in *B. theta* monocultures of the same age (Fig. 2b). Microscopy indicated that aggregates comprised intact *B. theta* with associated *M. smithii* (Fig. 2c and d) in addition to intact planktonic and extracellular matrix or dead cells (Fig. 2e and f). The accumulation of *M. smithii* cells in coculture lacking methanogenic substrates indicates that *B. theta* fermentation products are sufficient to support *M. smithii* growth. It should be noted that while lysed *B. theta* may provide metabolite precursors, *M. smithii* has an absolute requirement for acetate for acetyl-CoA biosynthesis and it is restricted to using H<sub>2</sub> and CO<sub>2</sub> and possibly formate as carbon and energy sources.

**Quantification of *B. theta* and *M. smithii* in coculture.** To determine if the interaction is solely a cross-feeding interaction or if *B. theta* also benefits from coculture with *M. smithii* during long-term cultivation with glucose as the sole carbon and energy

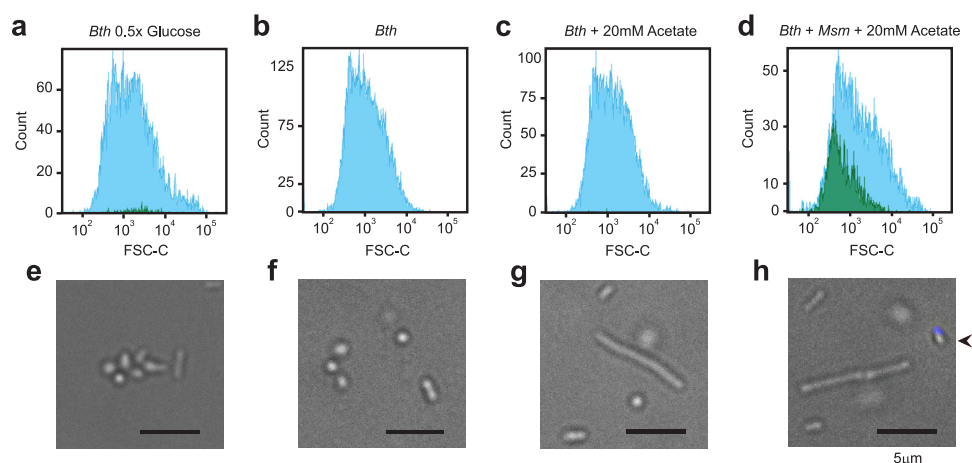


**FIG 3** Quantification of *B.theta* and *M. smithii* in cocultures using flow cytometry. (a to d) Cells were grown in defined medium for 9 days and counted by flow cytometry. The x axis reports forward scattering to quantify the size of the cell populations. Blue histogram indicates *B.theta* staining. Green histogram indicates *M. smithii* signal. (e to h) Cells from the same experiments as in panels a to d were visualized by transmission electron microscopy and UV fluorescence with a DAPI filter to detect *M. smithii* (arrow). Black bars indicate 5  $\mu\text{m}$  scale. (a and e) *B.theta* grown alone in 0.5 $\times$  glucose medium. (b and f) *B. theta* grown alone on glucose defined medium. (c and g) *B.theta* grown in defined medium supplemented with 20 mM acetate. (d and h) *B.theta* and *M. smithii* grown in coculture supplemented with 20 mM acetate.

source, the ratio of each organism in coculture populations was quantified using quantitative PCR (qPCR) and flow cytometry. We calculated cell ratios by qPCR by probing for the 16S rRNA-coding region of the genome. Between 4 and 9 days of coculture, there was no change in the coculture optical density, and the ratio of *B. theta* to *M. smithii* remained steady at 11.56 ( $\pm 3.03$ ) on day 4 to 14.25 ( $\pm 4.72$ ) on day 9 ( $P = 0.313$ ). To confirm the qPCR results, we also developed a flow cytometry assay to quantify changes in the population ratio according to cell wall staining and to measure cell aggregation. We found that when grown in the presence *M. smithii*, *B. theta* (Fig. 3b to d and f to h) forms larger cells or aggregates, which mimics the phenotype observed when *B. theta* is grown in rich medium with 0.5 $\times$  glucose (Fig. 3a and e). When 0.5 $\times$  glucose is provided, cultures deplete glucose carbon source and enter stationary phase more rapidly. Consistent with the qPCR data, after 4 days the ratio of planktonic *B. theta* to *M. smithii* cells was 10.97 ( $\pm 3.81$ ). These results suggest that *B. theta* and *M. smithii* reach balanced growth, in contrast to a purely cross-feeding interaction in which we would expect the ratios to transition from *B. theta*-dominated to *M. smithii*-dominated cultures over time. Culturing, microscopy, and quantification experiments suggest that *B. theta* forms irregular aggregates under limiting nutrient conditions that either passively “trap” or actively recruit *M. smithii*.

**Evidence for metabolic cross-feeding between *B. theta* and *M. smithii*.** *M. smithii* growth may be supported by *B. theta* fermentation products acetate, formate, and  $\text{H}_2$  plus  $\text{CO}_2$ . We next assessed the effect of acetate on cocultures, as acetate is required for *M. smithii* growth. Under these conditions, growth of *M. smithii* still requires  $\text{H}_2$  and  $\text{CO}_2$  provided by *B. theta*, as *M. smithii* cannot grow on acetate as an energy source. When cocultures were supplemented with 20 mM acetate, *B. theta* cells were larger and formed aggregates, and the relative proportion of *B. theta* to *M. smithii* decreased to 4.52 ( $\pm 1.56$ ) (Fig. 3d and h). The decrease in the relative proportion of *B. theta* to *M. smithii* with acetate supplementation is interpreted to suggest that acetate is growth-limiting for *M. smithii* in cocultures.

We hypothesized that if *B. theta* and *M. smithii* have a metabolic relationship, whether it be cross-feeding or syntrophy, then one or both of them may secrete unknown small molecules such as amino acids, bacteriocins, toxins, or quorum-sensing factors to promote growth of the other organism. We tested whether preconditioned medium may have a positive effect on growth of monocultures. In these experiments,

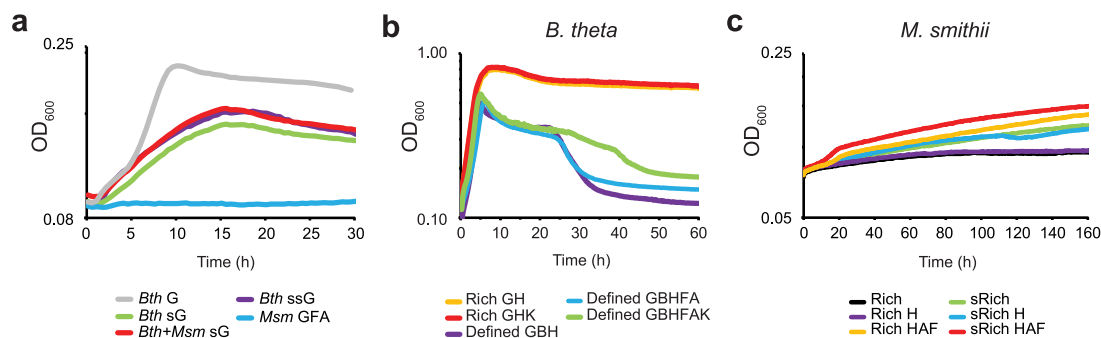


**FIG 4** Stimulation of *B. theta* and *M. smithii* growth by preconditioning or nutrient supplementation. (a) Growth of *B. theta* monocultures (*Bth*) in rich medium is enhanced by preconditioning with *M. smithii* (*Msm*;  $n = 8$ ). *Bth* G, *B. theta* monocultures grown on control glucose medium; *Bth* sG, growth of *B. theta* monocultures on glucose medium conditioned by *B. theta*; *Bth*+*Msm* sG, *B. theta* plus *M. smithii* cocultures grown on glucose medium conditioned by *B. theta* monoculture; *Bth* ssG, growth of *B. theta* monocultures on glucose medium preconditioned first by *B. theta* monoculture, then by *M. smithii* monoculture; *Msm* GFA, growth of *M. smithii* on rich medium control with glucose, formate, and acetate supplementation. (b) Lysis of *B. theta* monocultures in defined medium is delayed by the addition of vitamin  $K_3$ . (c) Growth of *M. smithii* monocultures on rich medium with glucose (Rich) is enhanced when medium is preconditioned by *B. theta* (sRich,  $n = 8$ ). Error bars have been omitted for clarity.  $OD_{600}$ , optical density at 600 nm; G, 0.5% glucose; B, vitamin  $B_{12}$ ; H, hematin; K, vitamin  $K_3$ ; F, 10 mM formate; A, 10 mM acetate.

media were preconditioned by inoculating with either *B. theta* or *M. smithii* monocultures and allowing the monoculture to grow to stationary phase before filter sterilizing with a 0.2- $\mu$ m filter to remove intact cells. When *B. theta* was grown on rich medium that had been preconditioned by *B. theta* monocultures, growth was slower and maximum optical density was decreased (Fig. 4a). When *B. theta* was grown on medium that had been sequentially preconditioned first by *B. theta* and then by *M. smithii*, cultures grew faster to a higher maximum optical density; however, the growth enhancement was not significant versus growth of *B. theta* on rich medium preconditioned by *B. theta* (Fig. 4a). *B. theta* and *M. smithii* cocultures grown on defined medium that had been preconditioned by *M. smithii* or *B. theta* monocultures grew similarly to *B. theta* cultures using medium that had been preconditioned by sequential culturing of *B. theta* and then *M. smithii* monocultures. These results suggest that when grown sequentially, *B. theta* depletes rich medium of one or more nutrients that are provided at a low level by *M. smithii*. In an attempt to identify nutrients that might improve growth of *B. theta*, we supplemented rich and defined medium with hematin, vitamin  $B_{12}$ , vitamin  $K_3$ , formate, and acetate. Growth experiments indicate that the lysis observed in rich medium was reduced by addition of hematin with vitamin K (Fig. 4b). In defined medium, vitamin  $B_{12}$ , hematin, formate, and acetate had no effect, but vitamin K improved growth (Fig. 4b). We also tested whether *M. smithii* growth is enhanced by rich medium preconditioned by *B. theta*. *M. smithii* was able to grow solely on rich medium preconditioned by *B. theta*, suggesting that molecules secreted by *B. theta* were responsible for stimulating *M. smithii* growth (Fig. 4c). *M. smithii* growth was further enhanced by adding hematin, acetate, and formate. However, the growth stimulation observed using preconditioned media was not as dramatic as the growth observed in cocultures (Fig. 1c and Fig. 2). Cross-feeding data indicated that a comprehensive systematic approach was needed to characterize the complex metabolic relationship between *B. theta* and *M. smithii* in coculture.

***B. theta* growth is inhibited by the presence of hydrogen gas, formate, and acetate.** To tease apart the metabolic interactions between *B. theta*, *M. smithii*, and the culture environment, we used a machine learning technique to analyze large-scale growth culture phenotype data. We assessed the growth of each organism alone and in coculture in 128 different combinations of culture media (2<sup>7</sup>). The combinatorial media recipes included or omitted the following nutrient components: 0.05% glucose, 10 mM acetate, 10 mM formate, 5.8 mM vitamin  $K_3$ , 0.0037  $\mu$ M vitamin  $B_{12}$ , and a mixture of 0.2 mM histidine and 0.02 mM hematin in the presence or absence of 5%  $H_2$  headspace gas. The optical densities of *B. theta*, *M. smithii*, and cocultures were

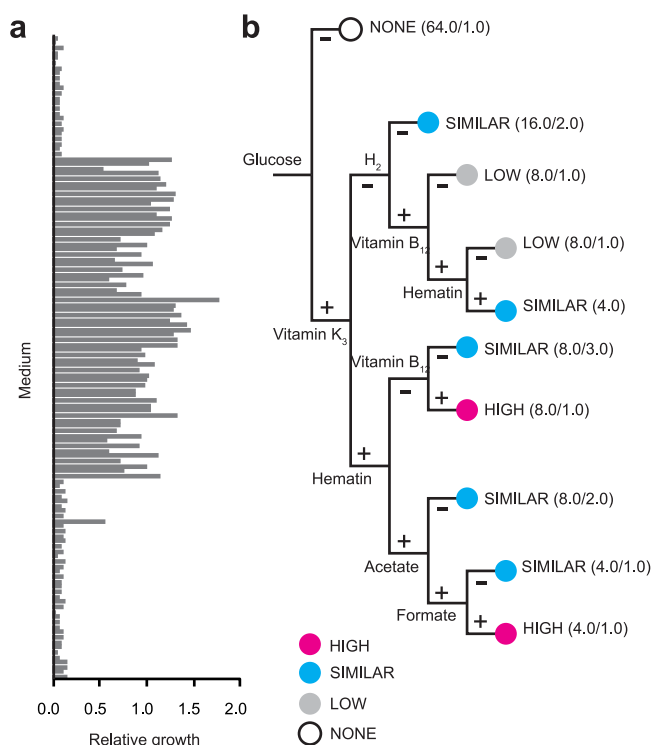


**FIG 5** Effect of medium composition on *B. theta* growth. Triplicate *B. theta* monocultures were grown in replicates of 8 on defined medium supplemented with 128 different combinations of glucose, vitamin B<sub>12</sub>, hematin, vitamin K<sub>3</sub>, acetate, formate, and a 5% H<sub>2</sub> atmosphere. Data across 3 experiments were compared to a positive control (glucose, hematin, vitamin B<sub>12</sub>, acetate, formate, and 5% H<sub>2</sub>) and combined. (a) *B. theta* growth relative to a positive control. (b) Decision tree representation of growth data relative to glucose, hematin, and vitamin B<sub>12</sub> control condition. The decision tree representation is read from left to right where each node represents one of the 7 nutrient conditions. The “-” path means the nutrient was not included, and the “+” path means it was included. As the path is traversed, the nutrients are additive. The values in parentheses represent how many total conditions are covered by that leaf, followed by how many are incorrectly classified by the model. Growth relative to the positive control is indicated as follows: open circles, no growth (NONE, <0.25); gray circles, low growth (LOW, ≥0.25, <0.75); blue circles, similar growth (SIMILAR, ≥0.75, <1.25); and pink circles, high growth (HIGH, ≥1.25).

measured after 1 day to capture maximal *B. theta* optical density, 7 days to capture slow-growing *B. theta* and maximal *M. smithii* optical density, and 14 days to measure culture stability after prolonged incubation. The same time points were observed to allow comparisons between monocultures and cocultures for every growth condition. To analyze and visualize these data, we utilized C4.5 decision trees to identify the relationships between nutrient factors in the culture medium (36). Decision trees draw branch nodes depending on whether the presence or absence of the factors (in this case, the provided nutrients) affects growth of the culture.

In defined medium, glucose was the only carbon source available to *B. theta* and was the primary determinant of growth (Fig. 5a). The structure of the decision tree suggests that the presence of hydrogen gas alone inhibits growth (Fig. 5b). Hydrogen gas inhibited *B. theta* growth up to 37.6% (Fig. 6a). When combined with acetate and formate supplementation, growth is decreased by 55% (supplemental material). Acetate and formate alone do not have a significant effect on growth of *B. theta* (Fig. 6a), although the tree suggests that the presence of acetate and formate in combination may increase growth under certain conditions. Interestingly, the tree indicates that the inhibition caused by H<sub>2</sub> is mitigated by the presence of vitamin K or a combination of vitamin B<sub>12</sub> and hematin/histidine (Fig. 5b). Additional experiments are needed to understand how this could be occurring, as inhibition of growth by hydrogen gas is not well understood in *B. theta*. *M. smithii* is unable to grow under conditions that favor *B. theta* unless hydrogen, formate, and acetate are present (Fig. 6c).



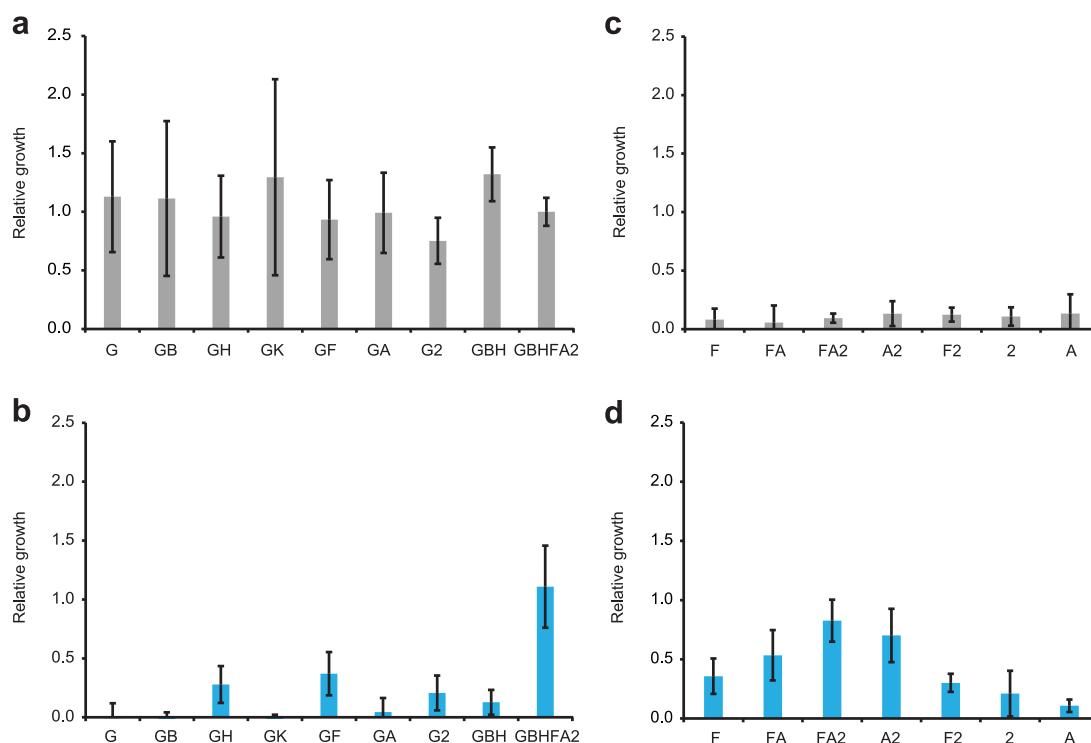


**FIG 6** Identification of defined medium that supports independent growth. (a and c) Growth of *B. theta* in dropout medium. (b and d) Growth of *M. smithii* in dropout medium. Data for each panel were obtained from triplicate biological and 8 technical replicates ( $n = 24$ ). Error bars represent standard deviation. G, 0.5% glucose; B, vitamin B<sub>12</sub>; H, hematin; K, vitamin K<sub>3</sub>; F, 10 mM formate; A, 10 mM acetate; 2, 5% H<sub>2</sub> atmosphere.

***M. smithii* grows best on a combination of glucose, vitamin B<sub>12</sub>, hematin, acetate, formate, and H<sub>2</sub> gas but depends on acetate for biomass.** As expected, *B. theta* is incapable of growth (Fig. 6b) under conditions that *M. smithii* prefers (Fig. 6d). *M. smithii* grew well in defined medium containing formate, acetate, and hydrogen, even with the addition of glucose, vitamin B<sub>12</sub>, and hematin (Fig. 6c). Overall, *M. smithii* was able to grow under a wider variety of conditions than *B. theta*, albeit to a lower maximum optical density (Fig. 7a). The decision tree for *M. smithii* suggests that acetate is the primary determinant for the growth of *M. smithii* (Fig. 7b). The presence of hydrogen or formate is necessary but not sufficient for growth (Fig. 6d). Both vitamin K<sub>3</sub> (menadione) and vitamin B<sub>12</sub> can inhibit *M. smithii* growth, but under certain circumstances vitamin B<sub>12</sub> rescues vitamin K inhibition and hematin can rescue vitamin B<sub>12</sub> inhibition (Fig. 7b).

**Dynamics of coculture phenotypes.** To compare the growth of the cocultures to the monocultures, growth was normalized to the control treatment that contains the necessary additive requirements for both organisms: glucose, hematin, vitamin B<sub>12</sub>, formate, acetate, and H<sub>2</sub>. Relative to that of the control, coculture growth closely resembles the *B. theta* monoculture tree after 1 day (Fig. 8a) but increasingly resembles *M. smithii* by day 7 through day 14 (Fig. 8bc). On day 1, glucose is the primary growth factor (Fig. 8a). By day 7, biomass is primarily linked to glucose catabolism, but acetate and hydrogen gas also influence coculture growth (Fig. 8b). By day 14, growth is dependent less on glucose and more on acetate, indicating increased importance of *M. smithii* in the coculture (Fig. 8c). However, the decision trees for the coculture do not directly mimic the monoculture trees. These data indicate that the metabolic relationship between *B. theta* and *M. smithii* is dynamic over a 2-week period and that coculture growth is not a simple additive relationship that can easily be predicted from monoculture data. This is consistent with observations made by others in which metabolism of diverse microbes is shaped by other members in a consortium (53, 54).

**The synergistic interaction index uncovers nutrient-dependent trophic interactions.** The complex growth patterns we observed suggested that under some conditions,

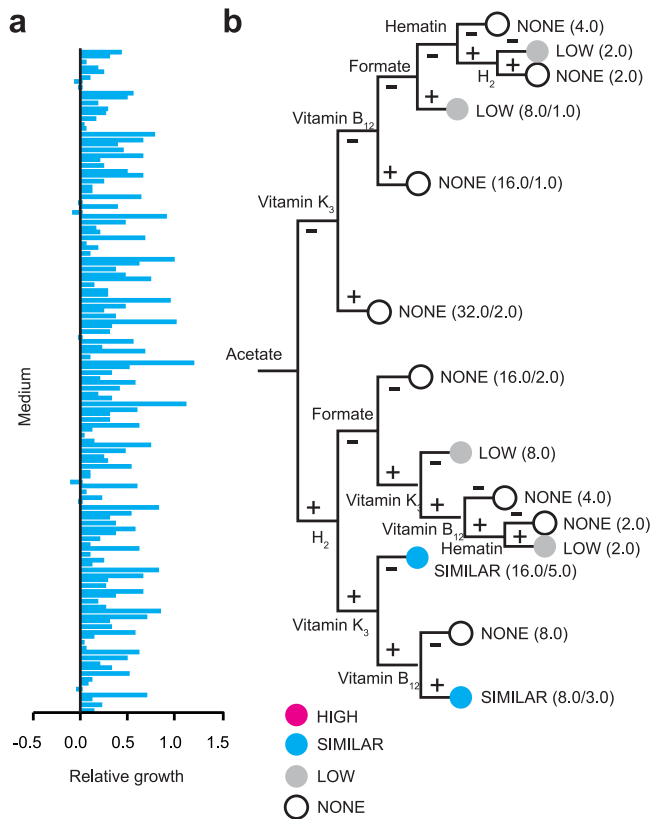


**FIG 7** Effect of medium composition on *M. smithii* growth. Triplicate *M. smithii* monocultures were grown in replicates of 8 on defined medium supplemented with 128 different combinations of glucose, vitamin B<sub>12</sub>, hematin, vitamin K<sub>3</sub>, acetate, formate, and a 5% H<sub>2</sub> atmosphere. Data across 3 experiments were compared to a positive control of acetate, formate, and 5% H<sub>2</sub> and combined. (a) *M. smithii* growth relative to a positive control. (b) Decision tree representation of growth data relative to H<sub>2</sub>, acetate control condition. Growth relative to the positive control is indicated as follows: open circles, no growth (NONE, <0.25); gray circles, low growth (LOW, ≥0.25, <0.75); blue circles, similar growth (SIMILAR, ≥0.75, <1.25); and pink circles, high growth (HIGH, ≥1.25).

*B. theta* and *M. smithii* could be growing independently, while in other culture media they may cross-feed each other and/or may compete for nutrients. We developed a synergistic interaction index to analyze the growth time course data (Fig. 9). Because *B. theta* will not grow without glucose, only the cases where glucose was supplemented were examined, and the synergistic interaction index (SI) was determined at 7 and 14 days (Fig. 10, supplemental material). The SI for the control condition was 1 on both days, indicating an additive mutualistic relationship between *B. theta* and *M. smithii* growth as expected (Table 2 and 3). After 7 days, two cocultures (glucose plus vitamin B<sub>12</sub> plus heme plus H<sub>2</sub> and glucose plus vitamin B<sub>12</sub> plus H<sub>2</sub>) had an SI of ≥1.5, indicating that the relative growth of the coculture was at least 1.5× that of the two monocultures together (supplemental material). One of these conditions (glucose plus vitamin B<sub>12</sub> plus H<sub>2</sub>) had an SI of 2.307, indicating coculture growth 2 times that of the monocultures together (Table 2 and 3). By 14 days, 7 cocultures had an SI of ≥1.5 with a maximum value of 2.36 for the glucose plus vitamin B<sub>12</sub> plus H<sub>2</sub> condition (Table 2 and 3). Cultures showing the highest indexes on day 14 were supplemented with vitamin B<sub>12</sub>, which is surprising because B<sub>12</sub> inhibited *M. smithii* growth in monoculture (Fig. 6b). One of the seven conditions with an SI of ≥1.5 included two fermentation products, acetate and hydrogen, and four cultures supplemented with acetate showed an increase of at least 0.5 SI units between days 7 and 14. Of the 11 cultures with day 14 SI of >1.25, 10 showed an increase from day 7 to day 14, likely indicating the differences in growth rates between *B. theta* and *M. smithii* and suggesting that depletion of glucose (and starvation of *B. theta*) is required for synergistic growth

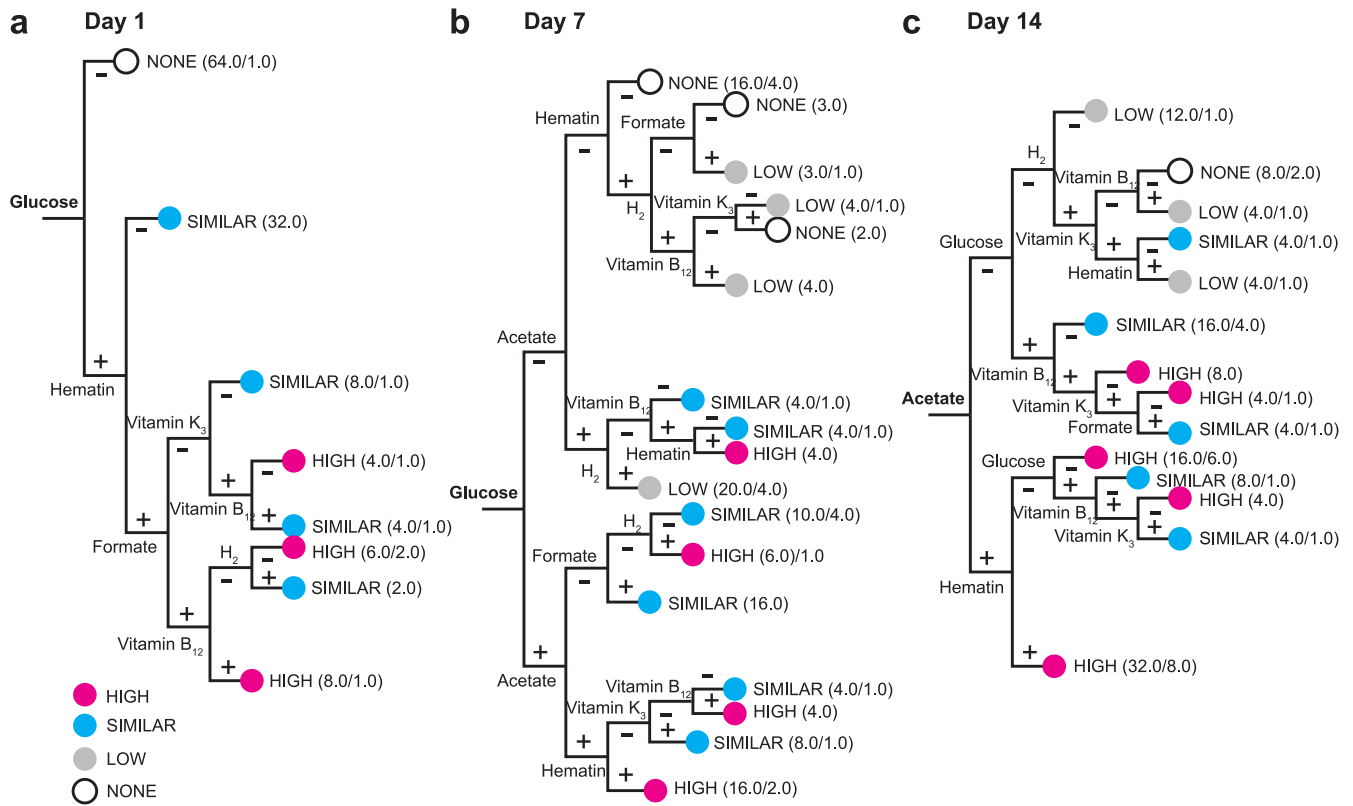


**FIG 8** Decision trees of coculture growth results. Triplicate *B. theta* plus *M. smithii* cocultures were grown in replicates of 8 on glucose defined medium supplemented with 64 different combinations of vitamin B<sub>12</sub>, hematin, vitamin K<sub>3</sub>, acetate, formate, and a 5% H<sub>2</sub> atmosphere. (a) Cocultures after 1 day of growth. (b) Cocultures after 7 days of growth. (c) Cocultures after 14 days of growth. Data were obtained from triplicate biological and eight technical replicates (*n* = 24). Growth relative to the positive control is indicated as follows: open circles, no growth (NONE, <0.25); gray circles, low growth (LOW, ≥0.25, <0.75); blue circles, similar growth (SIMILAR, ≥0.75, <1.25); and pink circles, high growth (HIGH, ≥1.25).

under these culture conditions. Measurement of SI after 7 days correlated very well with SI measured at 14 days with an *r*<sup>2</sup> value of 0.7922 (Fig. 10a). Twenty-four cultures had an SI of <0.75, suggesting the possibility of antagonistic inhibition or competition between *B. theta* and *M. smithii*. Of those 24 cultures, 20 saw a decrease in index from day 7 to day 14. Overall, synergistic growth was dependent on the availability of heme, vitamin B<sub>12</sub>, acetate, and hydrogen (Fig. 9).

**Synergistic growth is correlated with nutrient limitation and feedback inhibition.**

We noted that conditions indicating coculture synergy occurred when *B. theta* monocultures grew poorly. When the day 7 SI is compared to the growth of *B. theta* in monocultures under the same conditions, we observed a strong inverse correlation with an *r*<sup>2</sup> value of 0.6118 (Fig. 10b). In contrast, the day 7 SI was correlated only very weakly with *M. smithii* growth with an *r*<sup>2</sup> value of 0.0657 (Fig. 10c). The decision tree analysis (Fig. 8) shows that highest growth occurs when the coculture is supplemented with acetate, formate, and hematin. When cocultured, the data suggest that both organisms compete for hematin (Fig. 9c and d), especially when *M. smithii* growth is stimulated by added formate, acetate, and/or hydrogen (supplemental material).

**DISCUSSION**

Our study highlights the benefit of using an interdisciplinary approach to discern patterns of microbial growth as environmental conditions are varied. We have been able to adapt the use of decision trees from machine learning to parse through large-scale phenotype data to identify critical nutrient factors that contribute to growth. Machine learning decision trees are an unbiased tool to search for patterns in large-scale data to uncover hierarchy and interactions between variables. Here, we used optical density to measure culture growth as an output-dependent variable due to the

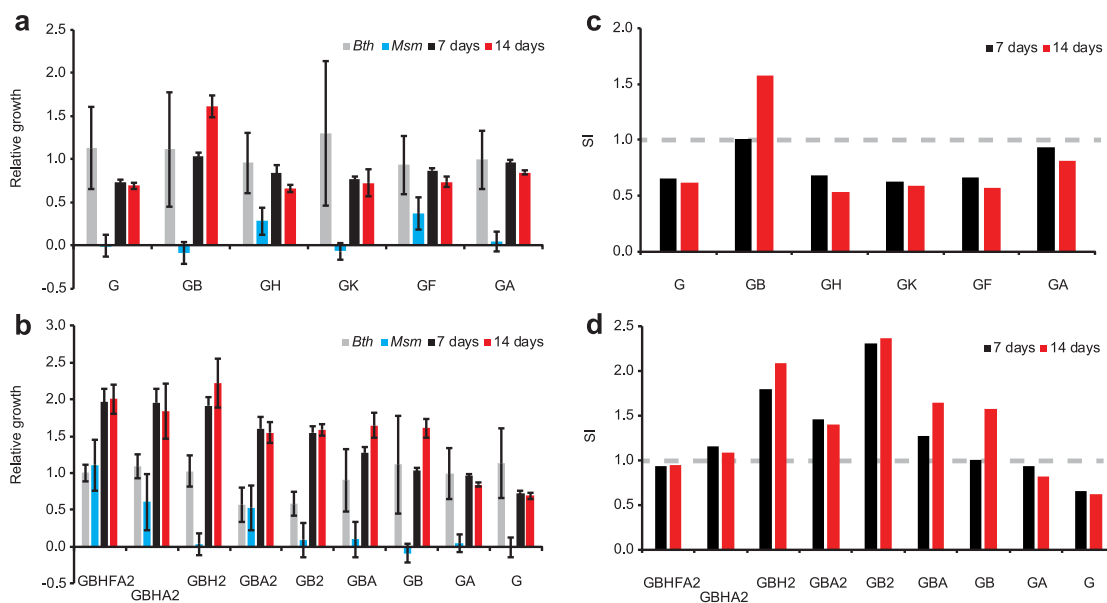


**FIG 9** Metabolic synergistic interaction index (SI). (a) Effect of nutrient supplementation on growth. (b) Effect of nutrient combinations on growth. (c and d) SI of conditions shown in panels a and b, respectively. An index of 1 (dotted gray line) indicates the null hypothesis where organisms grow independently in coculture. An index greater than 1 indicates that the relative growth of the coculture is greater than the sum of the monocultures, suggesting a syntrophic relationship. An index of less than one indicates a competitive or inhibitory effect. Error bars represent standard deviation from triplicate biological and eight technical replicates ( $n = 24$ ). G, 0.5% glucose; B, vitamin B<sub>12</sub>; H, heme; K, vitamin K<sub>3</sub>; F, 10 mM formate; A, 10 mM acetate; 2, 5% H<sub>2</sub> atmosphere.

ease of obtaining high-throughput data. However, decision trees can be adapted to use for any combination of dependent and independent variables in biological systems. This approach allowed us to ascertain patterns in growth phenotypes as well as emergent behaviors, in this case competition and synergistic growth, when two species are cocultured. We then developed a method to quantify these emergent behaviors in the form of a synergistic interaction index. Our approaches apply well to studying the interactions between microbes as diverse as the Gram-negative bacterium *B. theta* and the archaeal methanogen *M. smithii*. While we used endpoint optical density as an output parameter, which may mask phenotypes such as changes in cell size, shape, lysis, and aggregation, other complementary signals, such as 16S sequence or metatranscriptomic abundance, biomass, metabolites produced or consumed, or the rates of change of these signals, could theoretically be used instead with minimal adaptation. Likewise, while we constrained our study here to two organisms, with minor adjustment to account for number of species the approach could be retooled for more complex microbial communities.

A major consideration when studying complex microbial communities would be to use statistical sampling techniques such as BioSIMP (55) to develop technically and logistically feasible experiments that still retain a suitable confidence interval for

**TABLE 2** Synergistic interaction index statistics

Index range ( $I_i$ )	No. of treatments on day:	
	7	14
> 1.5	2	7
> 1.25	8	11
$0.75 \geq x \geq 1.25$	79	5
< 0.75	24	29
< 0.5	2	1

**TABLE 3** Synergistic interaction index statistics

Extrema	Index value ( $I_t$ ) on day:	
	7	14
Maximum	2.307	2.366
Minimum	0.376	0.397
Positive control <sup>a</sup>	0.928	0.950

<sup>a</sup>Defined medium supplemented with glucose, histidine and hematin, vitamin B<sub>12</sub>, formate, acetate, and H<sub>2</sub>. In this treatment, *B. theta* and *M. smithii* are provided nutrients for both to grow independently.

observed responses. BioSIMP involves using statistical sampling techniques to reduce the number of experiments required to uncover unexpected behavior/interactions in a biological system. For instance, instead of testing a full-factorial array of environmental conditions, statistical subsampling can be used to reduce the experiments by 50% or more to find which culture conditions can be expected to produce a growth effect of a certain magnitude. Precious resources in time, money, materials, and personnel can be devoted to more detailed mechanistic experiments that require full-factorial experimentation once “interesting” or “unexpected” results are identified for follow-up study.

The results of this study show that fermentation products secreted by *B. theta* are sufficient to support growth of *M. smithii* (Fig. 1c) and that *M. smithii* enhances growth of *B. theta* (as determined by growth curve data [Fig. 1c], microscopy [Fig. 2e], and qPCR experiments). One explanation for this result could be that *B. theta* becomes feedback inhibited by secreted metabolic by-products but in the presence of *M. smithii* the products are consumed, thus reducing growth inhibition. We showed in a previous study that the major fermentation products secreted by *B. theta* during growth on glucose suppress *B. theta* growth rates and alter metabolism, resulting in increased production of carbon dioxide and amino acids (52). *M. smithii* is capable of growing solely on the metabolites secreted by *B. theta* (Fig. 1c), and medium that has been sequentially conditioned first by *B. theta* and then by *M. smithii* supports higher *B. theta* biomass than medium that was preconditioned by *B. theta* alone (Fig. 4a). It is unknown what *M. smithii* might secrete besides methane, biomass, or intracellular metabolites such as heme or corrinoids released by lysed cells. Heme iron is a well-studied nutrient requirement, and bacteria have many heme acquisition mechanisms, such as siderophores and pathogenesis factors, that they synthesize to acquire iron for enzyme cofactor synthesis from the environment, from neighboring microbes, or from the host (56, 57). Corrinoids have also been shown to play a key role in several interspecies systems, and competition for B<sub>12</sub> is thought to be a significant factor that shapes human gut microbial community ecology (58). Our results show that *B. theta* is capable of growth in medium without supplemented heme or B<sub>12</sub> when grown in coculture with *M. smithii* presumably because *B. theta* can scavenge heme and corrinoids synthesized by *M. smithii*.

It is formally possible that *B. theta* and *M. smithii* secrete one or more unknown small molecules that are sensed as interspecies signals in addition to the central metabolic inter-

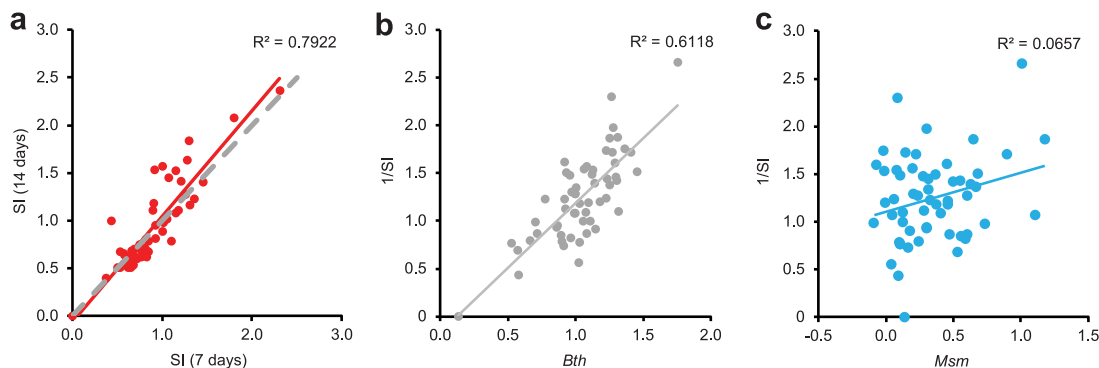


**FIG 10** Synergistic coculture growth is inversely related to *B. theta* growth. (a) Metabolic relationships are established and stable between 7 and 14 days in culture. (b) *B. theta* monoculture relative growth is inversely correlated with the 7-day synergistic interaction index (SI). (c) *M. smithii* monoculture relative growth is not correlated with the 7-day SI.

actions we tested in our treatments. Synergistic growth could be mediated by soluble and insoluble signals that may be expressed when *B. theta* is undergoing the starvation response. It is tempting to speculate that *B. theta* forms multicellular aggregates under starvation conditions to attract *M. smithii*, which would benefit from physical association with *B. theta* by allowing rapid mass transfer of hydrogen and acetate (Fig. 2). Intriguingly, these aggregates and the association of *M. smithii* with them statistically decreased when acetate was supplemented into the culture medium (Fig. 3), suggesting either that acetate induces signaling molecules by *B. theta* or that *M. smithii*, which requires exogenous acetate for growth, secretes molecule(s) that promote aggregate formation with *B. theta*. Whether the increase in *B. theta* growth is a result of secreted product from *M. smithii* or by the protective effect of removing inhibitory compounds is still to be decided. Additional experiments are needed to identify any attractants secreted by *B. theta* and/or *M. smithii* under conditions that favor and disfavor aggregate formation.

Finally, we developed a synergistic interaction index to score the likelihood that two or more organisms are growing synergistically or independently or are inhibiting each other. The index scores suggest that in some situations, the coculture is metabolically more efficient than expected from the biomass observed from independent monocultures. While the index does not identify the molecular mechanism of synergy or inhibition, by using a multicomponent culturing strategy and decision trees, we are able to discern patterns of coculture behavior that can lead to testable hypotheses. Our observations suggest that *B. theta* and *M. smithii* have a mutually beneficial syntrophic relationship when vitamin B<sub>12</sub> and hydrogen gas are provided and that they compete for heme when sufficient acetate, formate, and/or hydrogen gas are available for *M. smithii* to grow. Future experiments are needed to determine how *B. theta* and *M. smithii* compete for heme. We speculate that competition could proceed via passive mechanisms (autolysis, diffusion, and ATP-dependent transport) or by active processes using small molecules such as bacteriocins, toxins, quorum-sensing factors, or other mechanisms to obtain iron that have been discovered in other microbes (59–61).

## MATERIALS AND METHODS

**Strains and culturing conditions.** *B. theta* vpi-5482 (ATCC 29148, NB203) (62, 63) and *M. smithii* DSM0861 (ATCC 35061, NB215) (44) were used for the described studies. Strains were grown at 37°C in 18 mm by 150 mm Balch culture tubes under strict anaerobic conditions, in either a rich tryptone and yeast extract growth medium (TYG) or a defined medium. Previous work with *B. theta* utilized tryptone, yeast extract, and glucose medium (TYG) as a rich growth medium (15, 35, 64). Rich medium for *M. smithii* was also dependent on yeast extract (65, 66). Using TYG as a base, the recipes were combined to ensure growth for both organisms. *M. smithii* was initially grown in DSMZ *Methanobacterium* medium 119 (66) and then passaged into the modified rich medium supplemented with 10 mM formate and 10 mM acetate with 138 kPa 20% CO<sub>2</sub>, 80% H<sub>2</sub> headspace atmosphere. The defined medium was designed through a comparison of recipes (44, 45, 67–70). Rich medium contained tryptone peptone (10 g), Bacto yeast extract (5 g), 100 mM KPO<sub>4</sub> (pH 7.2), 40 mL TYG salts (0.5 g MgSO<sub>4</sub>·7H<sub>2</sub>O, 10 g NaHCO<sub>3</sub>, 2 g NaCl per L), 54.4 μM CaCl<sub>2</sub>, 1.4 μM FeSO<sub>4</sub>, 4 μM resazurin, 2.8 mM cysteine-HCl, and 25 μM Na<sub>2</sub>S per L. Defined medium contained 7.5 mM NH<sub>4</sub>SO<sub>4</sub>, 11.9 mM Na<sub>2</sub>CO<sub>3</sub>, 100 mM KPO<sub>4</sub> (pH 7.2), 14 μM FeSO<sub>4</sub>, 50 mL mineral salts (18 g NaCl, 0.53 g CaCl<sub>2</sub>·2H<sub>2</sub>O, 0.40 g MgCl<sub>2</sub>·6H<sub>2</sub>O, 0.20 g MnCl<sub>2</sub>·4H<sub>2</sub>O, 0.20 g CoCl<sub>2</sub>·6H<sub>2</sub>O per L), 4 μM resazurin, 2.8 mM cysteine-HCl, and 25 μM Na<sub>2</sub>S per L. When indicated, cultures were supplemented with 10 mM sodium acetate, 10 mM formate, 20 μM histidine and 2 μM heme, 3.7 nM vitamin B<sub>12</sub> (cyanocobalamin), or 5.8 mM vitamin K<sub>3</sub> (menadione). *B. theta* was supplemented with glucose to 0.05% (2.78 mM). Culture headspace was either 20% CO<sub>2</sub>, 80% N<sub>2</sub> or 5% H<sub>2</sub>, 20% CO<sub>2</sub>, 75% N<sub>2</sub> atmosphere at 138 kPa. *M. smithii* was grown on a rotary shaker operating at 45 rpm. *M. smithii* culture tubes were pressurized to 138 kPa with a 20% CO<sub>2</sub>, 80% H<sub>2</sub> gas mixture twice daily during growth curves or every 3 days for culture maintenance. Preliminary data suggested that vitamin K<sub>3</sub> may hinder *M. smithii* growth. *B. theta*/*M. smithii* cocultures were grown on or off the shaker under a 5% H<sub>2</sub>, 20% CO<sub>2</sub>, 75% N<sub>2</sub> atmosphere in rich or defined medium supplemented with glucose to 0.05% (2.78 mM).

**Growth curves.** *B. theta* and *M. smithii* were grown in 10 mL TYG and then transferred to media containing appropriate carbon sources and compounds. Growth in 18 mm by 150 mm anaerobic culture tubes was assessed by measuring changes in optical density at 600 nm using a Spec20D spectrophotometer modified with an 18 mm tube adapter. Growth in 96-well plates was assessed by measuring change in optical density at 600 nm using a Tecan Sunrise plate reader under a 5% H<sub>2</sub>, 20% CO<sub>2</sub>, 75% N<sub>2</sub> atmosphere.

**Microscopy.** Microscopy was performed using an EVOS FL auto cell imaging system with DAPI (4',6-diamidino-2-phenylindole), Texas Red, and green fluorescent protein LED light cubes in the University of Nebraska Morrison Microscopy Core Facility. *B. theta* and *M. smithii* were grown in medium containing an appropriate carbon source as described above. Cocultures were grown in defined medium with only

glucose as a carbon source. Five hundred-microliter samples were taken in an anaerobic atmosphere and stained with a combination of 5  $\mu\text{L}$  propidium iodide and 1  $\mu\text{L}$  SYTO 9 green per 500  $\mu\text{L}$  cells while remaining in anaerobic conditions. *M. smithii* coenzyme F<sub>420</sub> autofluorescence was viewed using a DAPI light cube (6, 38, 44, 71), propidium iodide with a Texas Red light cube, and Syto 9 green with a green fluorescent protein light cube.

**Flow cytometry.** Flow cytometry was performed using a BD Biosciences FACS Aria II flow cytometer (BD Biosciences) in the Nebraska Center for Biotechnology Flow Cytometry Core Facility. *B. theta* and *M. smithii* were grown anaerobically in rich medium supplemented with variable concentrations of glucose and sodium acetate over 4 and 9 days. Cell concentrations were recorded via optical density at 600 nm (OD<sub>600</sub>) and cultures were concentrated anaerobically via centrifugation at 500  $\times g$  for 10 min in a ThermoScientific Sorvall Legend Micro21 rotor, washed with phosphate-buffered saline (PBS; 137 mM NaCl, 2.7 mM KCl, 10 mM Na<sub>2</sub>HPO<sub>4</sub>, 1.8 mM KH<sub>2</sub>PO<sub>4</sub>), and resuspended to a concentration of  $\sim 1.0 \times 10^6$  cells per mL. Cells were dyed using LIVE/DEAD fixable yellow dead cell stain kit (Invitrogen) according to the protocol provided. Flow cytometry was performed exciting with a 405 nm laser until 10,000 events were recorded. Flow cytometry size standards were obtained from Fisher (1.0 to 15  $\mu\text{m}$  diameter; catalog number F13838). The gating control is shown in the supplemental material in Fig. S1.

**qPCR quantification.** *B. theta* and *M. smithii* were grown in rich media supplemented with glucose. Cultures were incubated at 37°C, and 1-mL samples were collected anaerobically on days 4 and 9 of growth. DNA was isolated from the cells using a phenol-chloroform extraction (72), and qPCR was performed on a Mastercycler RealPlex (2) instrument (Eppendorf) detecting SYBR green using probes for 16S regions of the *B. theta* (*B. theta* 16S fwd: 5'GGGATGCGTTCATTAGGC; *B. theta* 16S rev: 5'GGGACCTTCTCTCAGAACC) and *M. smithii* (*M. smithii* 16S fwd: 5'CGGCCGATTAGGTAGTTGGT; *M. smithii* 16S rev: 5'GTTCATCTCCGGGCTCTT) genomes. Threshold cycle (*C<sub>t</sub>*) values were normalized to input DNA, amplification efficiency, and the apparent number of genomes per cell. To account for variability in chromosome copy number between the two organisms, an apparent genome count was calculated by counting cells using a hemocytometer and carefully extracting the DNA from 1 mL of cells. The DNA quantity was measured via NanoDrop spectrophotometer (Thermo Scientific) and was divided by the genome size to calculate average number of genomes per cell, which would then be divided by the number of cells harvested in 1 mL.

**Dropout media preparation and growth assays.** For each biological replicate of the 7-component growth assay, dropout media were prepared that contained all combinations of vitamin K<sub>3</sub>, vitamin B<sub>12</sub>, formate, acetate, histidine-hematin, and glucose. Media were dispensed into 16 sterile 96-well culture plates, with two plates for each layout. One plate of each layout was kept under a 5% H<sub>2</sub>, 0.1% H<sub>2</sub>S, 20% CO<sub>2</sub>, 74.9% N<sub>2</sub> atmosphere, and the other was kept under 0.1% H<sub>2</sub>S, 20% CO<sub>2</sub>, 79.9% N<sub>2</sub>, resulting in 128 media combinations total.

*B. theta* and *M. smithii* were grown in 10 mL rich medium and used to inoculate prepared 96-well culture plates. For monocultures, 1:20 inocula (5  $\mu\text{L}$ ) of *B. theta*, 1:10 inocula (10  $\mu\text{L}$ ) of *M. smithii*, or a coculture of both were added to sample wells. The inoculum volumes for each strain were empirically determined to yield measurable culture turbidity within the 2-week experiment. One plate of each layout was placed in a 35°C anaerobic incubator with either 5% H<sub>2</sub>, 0.1% H<sub>2</sub>S, 20% CO<sub>2</sub>, 74.9% N<sub>2</sub> or 0.1% H<sub>2</sub>S, 20% CO<sub>2</sub>, 79.9% N<sub>2</sub> atmosphere. A Tecan Sunrise plate reader measured optical density at 600 nm after 7 days or 14 days under strict anaerobic conditions. The process was repeated for a total of three biological replicates.

**Growth data analysis.** The plate reader data were expected to contain errors due to splashing during handling, evaporation, and the formation of bubbles or cell clumps. Because each set of 8 samples or blanks contained similar contents, cells, and medium components, a normal distribution was assumed and Chauvenet's criterion was applied to eliminate statistical outliers in preparation for statistical and algorithmic analysis (73). Chauvenet's criterion specifies a probability band around the mean with a probability of  $1 - \frac{1}{2n}$ . Data within the band are retained, while data outside the band are considered outliers. For 8 samples, Chauvenet's criterion specifies a probability band that encompasses 93.8% of the population (equation 1):

$$P = 1 - \frac{1}{2 \cdot 8} = 0.937 \quad (1)$$

This corresponds to 1.863 standard deviations from the mean. Samples or blanks outside the band with a standard deviation greater than 1.863 were eliminated as outliers. After applying Chauvenet's criterion, differences in medium color were minimized by the subtraction of the mean value of the medium blanks from each sample. To allow data comparison across experiments, all samples were divided by the mean of a universal positive control grown in a H<sub>2</sub> atmosphere and containing glucose, vitamin B<sub>12</sub>, hematin, formate, and acetate. These samples were joined. To compare error across biological replicates, we assumed that the standard deviations should be approximately equal across data sets and calculated pooled variance  $s_p^2$  according to equation 2:

$$s_p^2 = \frac{\sum_{i=1}^k (n_i - 1)s_i^2}{\sum_{i=1}^k (n_i - 1)} \quad (2)$$

where  $n$  is the sample size of population  $i$  and  $s_i^2$  is the sample variance for population  $i$  or square of the standard deviation. Pooled standard error can then be calculated with equation 3:

$$SE_p = \sqrt{\sum_{i=1}^k \frac{s_p^2}{n_i}} \quad (3)$$

**Trees.** Decision trees are a divide-and-conquer machine learning technique that sorts data according to the data attributes that best divide the data. C4.5 decision trees were generated by running the data sets into a J28 classifier as previously described and drawn using Adobe Illustrator (36). BioSIMP software and tutorials can be found on the U.S. Department of Energy's Knowledge Base (KBase) (74). For analysis of monoculture data and coculture time course, sample averages were sorted into 4 buckets relative to a positive control containing glucose, hematin, vitamin B<sub>12</sub>, acetate, and formate and grown under a 5% H<sub>2</sub> atmosphere. Buckets related the growth to the positive control as follows: no growth (NONE, <0.25), low growth (LOW, ≥0.25, <0.75), similar growth (SIMILAR, ≥0.75, <1.25), and high growth (HIGH, ≥1.25).

**Synergistic interaction index calculations.** If all the cells in a coculture or consortium grow entirely independently of each other, with no interactions, the number of cells in the coculture ( $n_{\text{coculture}}$ ) would be equivalent to the sum of the number of monoculture cells grown under the same conditions, or in our case (equation 4):

$$n_{\text{coculture}} = n_{B.\text{theta}} + n_{M.\text{smithii}} \quad (4)$$

Because the optical density of the culture is directly proportional to the number of cells, we can compare the relative growth,  $R_{s,i}$ , of each culture of taxon  $s$  under culture condition  $i$  (equation 5):

$$R_{s,i} = \frac{\text{OD}_i}{\text{OD}_{\text{ctrl}}} \quad (5)$$

As long as each organism can grow independently in a positive control (ctrl) condition, an  $x$  component coculture of *B. theta* and *M. smithii* should have an overall growth that is an average of the monocultures (equation 6). Therefore, assuming independent growth within a coculture of *B. theta* and *M. smithii*, the relative growth,  $R$ , of a coculture can be calculated with equation 7.

$$R_{\text{coculture},i} = \frac{\text{OD}_{\text{coculture},i}}{\text{OD}_{\text{coculture},\text{ctrl}}} = \frac{1}{x} \cdot \sum_{s=1}^x R_{s,i} \quad (6)$$

$$R_{\text{coculture},i} = \frac{R_{B.\text{theta},i} + R_{M.\text{smithii},i}}{2} \quad (7)$$

This relationship will be true only if the growth of *B. theta* and that of *M. smithii* are independent of each other (null hypothesis). If the cells are interacting in a positive, syntrophic way, the coculture will contain more cells than the sum of the monocultures. If the cells are competitive, total growth will be inhibited and there will be fewer cells in the cocultures than expected. To express coculture interactions as a numerical value, we divided the observed coculture growth by the sum of the independent cultures, creating a synergistic interaction index for each culture condition,  $I_i$  (equation 8).

$$I_i = \frac{R_{B.\text{theta},i} + R_{M.\text{smithii},i}}{2R_{\text{coculture},i}} \quad (8)$$

A few caveats to this method should be considered depending on the organisms being studied. Under very high culture densities, the linear relationship between optical density and cell number is no longer valid, as the culture becomes increasingly opaque. In these situations, the index would be an underestimate of the coculture productivity. Another issue to keep in mind is that flocculation or aggregate formation would complicate experimental reproducibility. In spectrophotometric microplate readers, aggregates may be indicated when biological replicates produce signal variability depending on whether the beam hits an aggregate by chance. The result is high biological and technical variability that confounds statistical analysis. In either case, the index may be adapted by substituting biomass or another proxy growth measurement in place of OD variables in the above equations.

**Data availability.** Data from this study are available in the figures, tables, and supplemental material. The software tools developed for this study are available as user-friendly tutorials in the Department of Energy KBase at <https://narrative.kbase.us/narrative/19635>.

## SUPPLEMENTAL MATERIAL

Supplemental material is available online only.

**SUPPLEMENTAL FILE 1**, PDF file, 0.2 MB.

**SUPPLEMENTAL FILE 2**, XLSX file, 0.4 MB.

## ACKNOWLEDGMENTS

This material is based upon work supported by the National Science Foundation Grants (CCF 1901543 to M.B.C., IOS-1938948 to N.R.B., CCF-1816969 to M.P., and MCB-



1449014 to M.P. and N.R.B.), by an American Society for Microbiology Undergraduate Research Fellowship to M.D.S., and by the Nebraska Center for Integrated Biomolecular Communication (NIH National Institutes of General Medical Sciences P20-GM113126), and M.C. acknowledges PMI for support by UT-Battelle, LLC under contract no. DE-AC05-00OR22725 with the U.S. Department of Energy in the preparation and writing of the manuscript. Any opinions, findings, and conclusions or recommendations expressed in this material are those of the author(s) and do not necessarily reflect the views of the funding agencies.

This article was coauthored by UT-Battelle, LLC under contract no. DE-AC05-00OR22725 with the U.S. Department of Energy. The Department of Energy will provide public access to these results of federally sponsored research in accordance with the DOE public access plan (<http://energy.gov/downloads/doe-public-access-plan>).

## REFERENCES

- Flint HJ, Scott KP, Louis P, Duncan SH. 2012. The role of the gut microbiota in nutrition and health. *Nat Rev Gastroenterol Hepatol* 9:577–589. <https://doi.org/10.1038/nrgastro.2012.156>.
- Kim G, Deepinder F, Morales W, Hwang L, Weitsman S, Chang C, Gunsalus R, Pimentel M. 2012. *Methanobrevibacter smithii* is the predominant methanogen in patients with constipation-predominant IBS and methane on breath. *Dig Dis Sci* 57:3213–3218. <https://doi.org/10.1007/s10620-012-2197-1>.
- Chaudhary PP, Conway PL, Schlundt J. 2018. Methanogens in humans: potentially beneficial or harmful for health. *Appl Microbiol Biotechnol* 102:3095–3104. <https://doi.org/10.1007/s00253-018-8871-2>.
- Brown EG, Tanner CM, Goldman SM. 2018. The microbiome in neurodegenerative disease. *Curr Geriatr Rep* 7:81–91. <https://doi.org/10.1007/s13670-018-0240-6>.
- Palmer C, Bik EM, DiGiulio DB, Relman DA, Brown PO. 2007. Development of the human infant intestinal microbiota. *PLoS Biol* 5:e177. <https://doi.org/10.1371/journal.pbio.0050177>.
- Grine G, Boualam MA, Drancourt M. 2017. *Methanobrevibacter smithii*, a methanogen consistently colonising the newborn stomach. *Eur J Clin Microbiol Infect Dis* 36:2449–2455. <https://doi.org/10.1007/s10096-017-3084-7>.
- Bjursell MK, Martens EC, Gordon JL. 2006. Functional genomic and metabolic studies of the adaptations of a prominent adult human gut symbiont, *Bacteroides thetaiotaomicron*, to the suckling period. *J Biol Chem* 281:36269–36279. <https://doi.org/10.1074/jbc.M606509200>.
- Backhed F, Ley RE, Sonnenburg JL, Peterson DA, Gordon JL. 2005. Host-bacterial mutualism in the human intestine. *Science* 307:1915–1920. <https://doi.org/10.1126/science.1104816>.
- Savage DC. 1977. Microbial ecology of the gastrointestinal tract. *Annu Rev Microbiol* 31:107–133. <https://doi.org/10.1146/annurev.mi.31.100177.000543>.
- Yatsunenok T, Rey FE, Manary MJ, Trehan I, Dominguez-Bello MG, Contreras M, Magris M, Hidalgo G, Baldassano RN, Anokhin AP, Heath AC, Warner B, Reeder J, Kuczynski J, Caporaso JG, Lozupone CA, Lauber C, Clemente JC, Knights D, Knight R, Gordon JL. 2012. Human gut microbiome viewed across age and geography. *Nature* 486:222–227. <https://doi.org/10.1038/nature11053>.
- Stecher B, Hardt WD. 2011. Mechanisms controlling pathogen colonization of the gut. *Curr Opin Microbiol* 14:82–91. <https://doi.org/10.1016/j.mib.2010.10.003>.
- Buffie CG, Pamer EG. 2013. Microbiota-mediated colonization resistance against intestinal pathogens. *Nat Rev Immunol* 13:790–801. <https://doi.org/10.1038/nri3535>.
- Koropatkin NM, Cameron EA, Martens EC. 2012. How glycan metabolism shapes the human gut microbiota. *Nat Rev Microbiol* 10:323–335. <https://doi.org/10.1038/nrmicro2746>.
- Krajmalnik-Brown R, Ilhan ZE, Kang DW, DiBaise JK. 2012. Effects of gut microbes on nutrient absorption and energy regulation. *Nutr Clin Pract* 27:201–214. <https://doi.org/10.1177/0885433611436116>.
- Wexler HM. 2007. Bacteroides: the good, the bad, and the nitty-gritty. *Clin Microbiol Rev* 20:593–621. <https://doi.org/10.1128/CMR.00008-07>.
- Menni C, Jackson MA, Pallister T, Steves CJ, Spector TD, Valdes AM. 2017. Gut microbiome diversity and high-fibre intake are related to lower long-term weight gain. *Int J Obes* 41:1099–1105. <https://doi.org/10.1038/ijo.2017.66>.
- Round JL, Mazmanian SK. 2009. The gut microbiota shapes intestinal immune responses during health and disease. *Nat Rev Immunol* 9:313–323. <https://doi.org/10.1038/nri2515>.
- Hooper LV, Gordon JL. 2001. Commensal host-bacterial relationships in the gut. *Science* 292:1115–1118. <https://doi.org/10.1126/science.1058709>.
- Nicholson JK, Holmes E, Kinross J, Burcelin R, Gibson G, Jia W, Pettersson S. 2012. Host-gut microbiota metabolic interactions. *Science* 336:1262–1267. <https://doi.org/10.1126/science.1223813>.
- Louis P, Hold GL, Flint HJ. 2014. The gut microbiota, bacterial metabolites and colorectal cancer. *Nat Rev Microbiol* 12:661–672. <https://doi.org/10.1038/nrmicro3344>.
- Carbonero F, Benefiel AC, Gaskins HR. 2012. Contributions of the microbial hydrogen economy to colonic homeostasis. *Nat Rev Gastroenterol Hepatol* 9:504–518. <https://doi.org/10.1038/nrgastro.2012.85>.
- Parekh PJ, Balart LA, Johnson DA. 2015. The influence of the gut microbiome on obesity, metabolic syndrome and gastrointestinal disease. *Clin Transl Gastroenterol* 6:e91. <https://doi.org/10.1038/ctg.2015.16>.
- Fernandes J, Su W, Rahat-Rozenbloom S, Wolever TM, Comelli EM. 2014. Adiposity, gut microbiota and faecal short chain fatty acids are linked in adult humans. *Nutr Diabetes* 4:e121. <https://doi.org/10.1038/nutd.2014.23>.
- Wilder-Smith CH, Olesen SS, Materna A, Drewes AM. 2018. Breath methane concentrations and markers of obesity in patients with functional gastrointestinal disorders. *United European Gastroenterol J* 6:595–603. <https://doi.org/10.1177/2050640617744457>.
- Zhao L. 2013. The gut microbiota and obesity: from correlation to causality. *Nat Rev Microbiol* 11:639–647. <https://doi.org/10.1038/nrmicro3089>.
- Sartor RB. 2008. Microbial influences in inflammatory bowel diseases. *Gastroenterology* 134:577–594. <https://doi.org/10.1053/j.gastro.2007.11.059>.
- Halfvarson J, Brislawn CJ, Lamendella R, Vazquez-Baeza Y, Walters WA, Bramer LM, D'Amato M, Bonfiglio F, McDonald D, Gonzalez A, McClure EE, Dunkleberger MF, Knight R, Jansson JK. 2017. Dynamics of the human gut microbiome in inflammatory bowel disease. *Nat Microbiol* 2:17004. <https://doi.org/10.1038/nmicrobiol.2017.4>.
- Russell SL, Gold MJ, Hartmann M, Willing BP, Thorson L, Wlodarska M, Gill N, Blanchet MR, Mohn WW, McNagny KM, Finlay BB. 2012. Early life antibiotic-driven changes in microbiota enhance susceptibility to allergic asthma. *EMBO Rep* 13:440–447. <https://doi.org/10.1038/embor.2012.32>.
- Hooper LV, Littman DR, Macpherson AJ. 2012. Interactions between the microbiota and the immune system. *Science* 336:1268–1273. <https://doi.org/10.1126/science.1223490>.
- Ghavami SB, Rostami E, Sephay AA, Shahrokh S, Balaii H, Aghdaei HA, Zali MR. 2018. Alterations of the human gut *Methanobrevibacter smithii* as a biomarker for inflammatory bowel diseases. *Microb Pathog* 117:285–289. <https://doi.org/10.1016/j.micpath.2018.01.029>.
- Milani C, Ferrario C, Turroni F, Duranti S, Mangifesta M, van Sinderen D, Ventura M. 2016. The human gut microbiota and its interactive connections to diet. *J Hum Nutr Diet* 29:539–546. <https://doi.org/10.1111/jhn.12371>.
- Sommer F, Backhed F. 2013. The gut microbiota—masters of host development and physiology. *Nat Rev Microbiol* 11:227–238. <https://doi.org/10.1038/nrmicro2974>.
- Huitema MJD, Schenk GJ. 2018. Insights into the mechanisms that may clarify obesity as a risk factor for multiple sclerosis. *Curr Neurol Neurosci Rep* 18:18. <https://doi.org/10.1007/s11910-018-0827-5>.
- Basseri RJ, Basseri B, Pimentel M, Chong K, Youdim A, Low K, Hwang L, Soffer E, Chang C, Mathur R. 2012. Intestinal methane production in obese individuals is associated with a higher body mass index. *Gastroenterol Hepatol (NY)* 8:22–28.
- Samuel BS, Gordon JL. 2006. A humanized gnotobiotic mouse model of host-archaeal-bacterial mutualism. *Proc Natl Acad Sci U S A* 103:10011–10016. <https://doi.org/10.1073/pnas.0602187103>.

36. Cashman M, Catlett JL, Cohen MB, Buan NR, Sakkaff Z, Pierobon M, Kelley CA. 2017. BioSIMP: using software testing techniques for sampling and inference in biological organisms, p 2–8. 2017 IEEE/Acm 12th International Workshop on Software Engineering for Science (Se4science). IEEE Press, Buenos Aires, Argentina. <https://doi.org/10.1109/Se4science.2017.9>.
37. Sonnenburg JL, Chen CT, Gordon JI. 2006. Genomic and metabolic studies of the impact of probiotics on a model gut symbiont and host. *PLoS Biol* 4:e413. <https://doi.org/10.1371/journal.pbio.0040413>.
38. Demonfort Nkamga V, Henrissat B, Drancourt M. 2017. Archaea: essential inhabitants of the human digestive microbiota. *Human Microbiome J* 3: 1–8. <https://doi.org/10.1016/j.humic.2016.11.005>.
39. Miller TL, Wolin MJ. 1982. Enumeration of *Methanobrevibacter smithii* in human feces. *Arch Microbiol* 131:14–18. <https://doi.org/10.1007/BF00451492>.
40. Gill SR, Pop M, Deboy RT, Eckburg PB, Turnbaugh PJ, Samuel BS, Gordon JI, Relman DA, Fraser-Liggett CM, Nelson KE. 2006. Metagenomic analysis of the human distal gut microbiome. *Science* 312:1355–1359. <https://doi.org/10.1126/science.1124234>.
41. Dridi B, Henry M, El Khechine A, Raoult D, Drancourt M. 2009. High prevalence of *Methanobrevibacter smithii* and *Methanosphaera stadtmanae* detected in the human gut using an improved DNA detection protocol. *PLoS One* 4:e7063. <https://doi.org/10.1371/journal.pone.0007063>.
42. Hansen EE, Lozupone CA, Rey FE, Wu M, Guruge JL, Narra A, Goodfellow J, Zaneveld JR, McDonald DT, Goodrich JA, Heath AC, Knight R, Gordon JI. 2011. Pan-genome of the dominant human gut-associated archaeon, *Methanobrevibacter smithii*, studied in twins. *Proc Natl Acad Sci U S A* 108 Suppl 1:4599–4606. <https://doi.org/10.1073/pnas.1000071108>.
43. Million M, Maraninchi M, Henry M, Armougoum F, Richet H, Carrieri P, Valero R, Raccach D, Viallet B, Raoult D. 2012. Obesity-associated gut microbiota is enriched in *Lactobacillus reuteri* and depleted in *Bifidobacterium animalis* and *Methanobrevibacter smithii*. *Int J Obes (Lond)* 36: 817–825. <https://doi.org/10.1038/ijo.2011.153>.
44. Miller TL, Wolin MJ, Conway de Macario E, Macario AJ. 1982. Isolation of *Methanobrevibacter smithii* from human feces. *Appl Environ Microbiol* 43: 227–232. <https://doi.org/10.1128/aem.43.1.227-232.1982>.
45. Samuel BS, Hansen EE, Manchester JK, Coutinho PM, Henrissat B, Fulton R, Latreille P, Kim K, Wilson RK, Gordon JI. 2007. Genomic and metabolic adaptations of *Methanobrevibacter smithii* to the human gut. *Proc Natl Acad Sci U S A* 104:10643–10648. <https://doi.org/10.1073/pnas.0704189104>.
46. Morris BE, Henneberger R, Huber H, Moissl-Eichinger C. 2013. Microbial syntrophy: interaction for the common good. *FEMS Microbiol Rev* 37: 384–406. <https://doi.org/10.1111/1574-6976.12019>.
47. Sieber JR, McInerney MJ, Gunsalus RP. 2012. Genomic insights into syntrophy: the paradigm for anaerobic metabolic cooperation. *Annu Rev Microbiol* 66:429–452. <https://doi.org/10.1146/annurev-micro-090110-102844>.
48. McInerney MJ, Sieber JR, Gunsalus RP. 2009. Syntrophy in anaerobic global carbon cycles. *Curr Opin Biotechnol* 20:623–632. <https://doi.org/10.1016/j.copbio.2009.10.001>.
49. Kouzuma A, Kato S, Watanabe K. 2015. Microbial interspecies interactions: recent findings in syntrophic consortia. *Front Microbiol* 6:477. <https://doi.org/10.3389/fmicb.2015.00477>.
50. Stams AJ, Plugge CM. 2009. Electron transfer in syntrophic communities of anaerobic bacteria and archaea. *Nat Rev Microbiol* 7:568–577. <https://doi.org/10.1038/nrmicro2166>.
51. Stolyar S, Van Dien S, Hillesland KL, Pinel N, Lie TJ, Leigh JA, Stahl DA. 2007. Metabolic modeling of a mutualistic microbial community. *Mol Syst Biol* 3:92. <https://doi.org/10.1038/msb4100131>.
52. Catlett JL, Catazaro J, Cashman M, Carr S, Powers R, Cohen MB, Buan NR. 2020. Metabolic feedback inhibition influences metabolite secretion by the human gut symbiont *Bacteroides thetaiotaomicron*. *mSystems* 5. <https://doi.org/10.1128/mSystems.00252-20>.
53. Heyse J, Buysschaert B, Props R, Rubbens P, Skirtach AG, Waegeman W, Boon N. 2019. Coculturing bacteria leads to reduced phenotypic heterogeneities. *Appl Environ Microbiol* 85. <https://doi.org/10.1128/AEM.02814-18>.
54. Grant MA, Kazamia E, Cicuta P, Smith AG. 2014. Direct exchange of vitamin B12 is demonstrated by modelling the growth dynamics of algal-bacterial cocultures. *ISME J* 8:1418–1427. <https://doi.org/10.1038/ismej.2014.9>.
55. Cashman M, Catlett JL, Cohen MB, Buan NR, Sakkaff Z, Pierobon M, Kelley CA. 2017. BioSIMP: using software testing techniques for sampling and inference in biological organisms, p 2–8. Proceedings of the 12th International Workshop on Software Engineering for Science. IEEE Press, Buenos Aires, Argentina.
56. Wooldridge KG, Williams PH. 1993. Iron uptake mechanisms of pathogenic bacteria. *FEMS Microbiol Rev* 12:325–348. <https://doi.org/10.1111/j.1574-6976.1993.tb00026.x>.
57. Richard KL, Kelley BR, Johnson JG. 2019. Heme uptake and utilization by Gram-negative bacterial pathogens. *Front Cell Infect Microbiol* 9:81. <https://doi.org/10.3389/fcimb.2019.00081>.
58. Degnan PH, Taga ME, Goodman AL. 2014. Vitamin B12 as a modulator of gut microbial ecology. *Cell Metab* 20:769–778. <https://doi.org/10.1016/j.cmet.2014.10.002>.
59. Zhu W, Winter MG, Spiga L, Hughes ER, Chanin R, Mulgaonkar A, Pennington J, Maas M, Behrendt CL, Kim J, Sun X, Beiting DP, Hooper LV, Winter SE. 2020. Xenosiderophore utilization promotes *Bacteroides thetaiotaomicron* resilience during colitis. *Cell Host Microbe* 27:376–388.e378. <https://doi.org/10.1016/j.chom.2020.01.010>.
60. Zafar H, Saier MH, Jr. 2018. Comparative genomics of transport proteins in seven *Bacteroides* species. *PLoS One* 13:e0208151. <https://doi.org/10.1371/journal.pone.0208151>.
61. Lurie-Weinberger MN, Peeri M, Gophna U. 2012. Contribution of lateral gene transfer to the gene repertoire of a gut-adapted methanogen. *Genomics* 99:52–58. <https://doi.org/10.1016/j.ygeno.2011.10.005>.
62. Cato EP, Johnson JL. 1976. Reinstatement of species rank for *Bacteroides* -Fragilis, *Bacteroides*-Ovatus, *Bacteroides*-Distans, *Bacteroides*-Thetaiotaomicron, and *Bacteroides*-Vulgatus - designation of neotype strains for *Bacteroides*-Fragilis (Veillon and Zuber) Castellani and Chalmers and *Bacteroides*-Thetaiotaomicron (Distaso) Castellani and Chalmers. *Int J Syst Bacteriol* 26:230–237. <https://doi.org/10.1099/00207713-26-2-230>.
63. Kotarski SF, Salyers AA. 1984. Isolation and characterization of outer membranes of *Bacteroides thetaiotaomicron* grown on different carbohydrates. *J Bacteriol* 158:102–109. <https://doi.org/10.1128/jb.158.1.102-109.1984>.
64. Bacic MK, Smith CJ. 2008. Laboratory maintenance and cultivation of bacteroides species. *Curr Protoc Microbiol* Chapter 13:Unit 13C 11. <https://doi.org/10.1002/9780471729259.mc13c01s9>.
65. Khelaifa S, Raoult D, Drancourt M. 2013. A versatile medium for cultivating methanogenic archaea. *PLoS One* 8:e61563. <https://doi.org/10.1371/journal.pone.0061563>.
66. DSMZ. 2017. 119. Methanobacterium medium. List of media for microorganisms. DSMZ, Braunschweig, Germany. <https://www.dsmz.de/collection/catalogue/microorganisms/culture-technology/list-of-media-for-microorganisms>.
67. Varel VH, Bryant MP. 1974. Nutritional features of *Bacteroides fragilis* subsp. *fragilis*. *Appl Microbiol* 28:251–257. <https://doi.org/10.1128/am.28.2.251-257.1974>.
68. Balch WE, Fox GE, Magrum LJ, Woese CR, Wolfe RS. 1979. Methanogens: reevaluation of a unique biological group. *Microbiol Rev* 43:260–296. <https://doi.org/10.1128/mr.43.2.260-296.1979>.
69. Balch WE, Wolfe RS. 1979. Specificity and biological distribution of coenzyme M (2-mercaptoethanesulfonic acid). *J Bacteriol* 137:256–263. <https://doi.org/10.1128/jb.137.1.256-263.1979>.
70. Sowers KR, Boone JE, Gunsalus RP. 1993. Disaggregation of *Methanosarcina* spp. and growth as single cells at elevated osmolarity. *Appl Environ Microbiol* 59:3832–3839. <https://doi.org/10.1128/aem.59.11.3832-3839.1993>.
71. Peck MW. 1989. Changes in concentrations of coenzyme F420 analogs during batch growth of *Methanosarcina barkeri* and *Methanosarcina mazei*. *Appl Environ Microbiol* 55:940–945. <https://doi.org/10.1128/aem.55.4.940-945.1989>.
72. Sambrook J, Russell DW. 2006. Purification of nucleic acids by extraction with phenol:chloroform. *CSH Protoc* 2006:pdb.prot4455. <https://doi.org/10.1101/pdb.prot4455>.
73. Taylor JR. 1997. An introduction to error analysis: the study of uncertainties in physical measurements. University Science Books, Sausalito, CA.
74. Arkin AP, Cottingham RW, Henry CS, Harris CS, Stevens RL, Maslov S, Dehal P, Ware D, Perez F, Canon S, Sneddon MW, Henderson ML, Riehl WJ, Murphy-Olson D, Chan SY, Kamimura RT, Kumari S, Drake MM, Brettin TS, Glass EM, Chivian D, Gunter D, Weston DJ, Allen BH, Baumohl J, Best AA, Bowen B, Brenner SE, Bun CC, Chandonia JM, Chia JM, Colasanti R, Conrad N, Davis JJ, Davison BH, DeJongh M, Devoid S, Dietrich E, Dubchak I, Edirisinghe JN, Fang G, Faria JP, Frybarger PM, Gerlach W, Gerstein M, Greiner A, Gurtowski J, Haun HL, He F, Jain R, et al. 2018. KBase: the United States Department of Energy Systems biology knowledgebase. *Nat Biotechnol* 36:566–569. <https://doi.org/10.1038/nbt.4163>.